American Mineralogist, Volume 92, pages 518–524, 2007

Dissolution of the (001) surface of galena: An in situ assessment of surface speciation by fluid-cell micro-Raman spectroscopy

Giovanni De Giudici,[1,*] Piercarlo Ricci,[2] Pierfranco Lattanzi,[1,3] and Alberto Anedda[2,3]

[1]Dipartimento di Scienze della Terra, Università degli Studi di Cagliari, via Trentino 51, I-09127 Cagliari, Italy
[2]Dipartimento di Fisica, Università degli Studi di Cagliari, Cittadella di Monserrato, S.S. 554, I-09042 Monserrato (CA), Italy
[3]Laboratorio LIMINA, Università degli Studi di Cagliari, Cittadella di Monserrato, S.S. 554, I-09042 Monserrato (CA), Italy

Abstract

The chemical evolution of the galena (001) cleavage surface dissolving in oxygen-saturated solutions was investigated by fluid-cell micro-Raman Spectroscopy (μRS) and solution chemistry. In this novel design of μRS apparatus, the solution in the fluid cell is continuously renewed. A fairly thick (several tens to hundreds of nanometers) layer forms at the galena surface in solutions with pH between 1 and 5.8. This surface layer is composed of Pb oxides, sulfates, and metastable species of sulfur. Native sulfur forms at pH 1 and 4.6, but is not a predominant surface species at pH 5.8. Dissolution rates, measured by solution chemistry, decrease with pH and reaction time. The formation of Pb oxides in these experiments at such low pH values contrasts with thermodynamic predictions based on properties at the macroscale (bulk solution).

The in situ assessment of surface speciation confirms that sulfur can partially oxidize at the interface, and indicates that this process of sulfur oxidation depends on pH. We propose that sulfur oxidation may take place, at least partially, during the reaction of dissolved molecular oxygen with S atoms at the galena surface, or in the immediate vicinity. After this first step of reaction, oxygen combines with Pb ions to form Pb oxide at the interface.

Keywords: Surface speciation, in situ investigation, galena, surface dissolution

Introduction

Galena (PbS) is a mineral of both economic and environmental importance. Its dissolution has been extensively studied (e.g., De Giudici et al. 2005, and references therein) by means of several diverse techniques such as bulk reaction, atomic force (AFM) and scanning tunneling (STM) microscopy, electrochemistry, X-ray photoelectron spectroscopy (XPS), and Fourier-transform (FTIR) and attenuated total reflection (ATR) infrared spectroscopy. Evidence from these studies, ranging from bulk to micro- and nanoscale, from morphological to compositional, from ex situ to in situ, and from surface to bulk, is partly equivocal and open to debate (e.g., Chernyshova 2003). For instance, XPS investigations indicate that microscopic secondary products can correspond to sulfate, Pb hydroxides, Pb oxides, and Pb-deficient galena surfaces (e.g., Fornasiero et al. 1994). On the other hand, during the process of oxidation from sulfide to sulfate at galena surfaces, several thermodynamically unstable species can be kinetically favored, namely polysulfides and sulfoxy anions. However, these chemical species have short lifetimes and are sensitive to experimental conditions (Nowak and Laajalehto 2000). Fluid-cell atomic force microscopy (AFM) gives clear evidence for the appearance of nanometer-sized phases at a galena surface dissolving in acidic and oxygen-saturated solutions (De Giudici and Zuddas 2001; Cama et al. 2005; Stack et al. 2004; Mikhlin et al. 2005; and references therein). Despite this fairly large body of literature, both the structure and the composition of galena surface coatings are still poorly constrained.

In an early investigation based on factor-group analysis, Ferraro (1975) predicted that galena (and other rock-salt structure minerals) should have no Raman active vibrational modes, and therefore cannot be analyzed by Raman spectroscopy. More recently, several experimental investigations determining Raman spectra of metal sulfides supported this idea (Mernagh and Trudu 1993; Shapter et al. 2000). In contrast, however, a growing body of literature provides evidence for first-order and second-order Raman spectra of galena (Smith et al. 2002, and references therein). Most of these Raman investigations of the galena surface are dominantly of a technical nature, dealing, for example, with flotation problems (see Andreev and Barzev 2003; Chernyshova 2003, and literature therein).

A novel experiment using in situ micro-Raman spectroscopy (μRS) is presented in this work. The surface speciation at the galena (001) surface was investigated during dissolution in an oxygen-saturated solution at different pH values (ranging from 1 to 5.8, in HCl). The overall rates of galena dissolution in the μRS-fluid-cell are measured by solution chemistry. Results are compared with those obtained by previous AFM, bulk solution, and XPS studies on the same mineral (De Giudici and Zuddas 2001; De Giudici et al. 2005). The in-situ assessment of surface speciation is then compared to other literature data.

* E-mail: gbgiudic@unica.it

0003-004X/07/0004–518$05.00/DOI: 10.2138/am.2007.2181

Experimental methods

A large galena crystal from the Iglesiente mining district (Sardinia, Italy) was selected for this study. Fragments of the same specimen were used in previous investigations (De Giudici and Zuddas 2001; De Giudici et al. 2005). Previous bulk X-ray fluorescence analyses indicated trace impurities of Zn, Fe, and Cu (≤0.2 at%). Apart from rare inclusions of chalcopyrite and silver (determined by Raman spectroscopy), these impurities are not concentrated in recognizable microscopic phases over the analyzed sample surface. Upon careful cleaving in the laboratory, small grains of regular cubic form were obtained and used for the experiments. For each run, a freshly cleaved sample was mounted in the fluid cell.

The fluid cell used for in situ micro-Raman spectroscopy (μRS) was made of polyvinyl chloride (PVC). The galena fragment was mounted on the bottom of the cell, with the top of the cell left open, to allow both microscope focusing and exchange between solution and the ambient atmosphere. Basically, this flow-through reactor replicates the fluid cell used in previous AFM experiments (see De Giudici and Zuddas 2001 for more details). The flow rate, Q, was controlled by a peristaltic pump (Gilson Minipulse III) set to value of 1 mL/min. To ensure that the interacting solution was always undersaturated with respect to both Pb sulfide and Pb sulfate, the pumping was maintained at this rate so that complete exchange of product fluid for fresh reactant fluid in the reaction vessel occurred approximately every three minutes.

The reactant solutions were made by adding the desired amount of hydrochloric acid (suprapur) to deionized water. Solution pH was measured after pH calibration against a NIST buffer and did not change measurably after the reaction with the galena surface. The experimental oxygen partial pressure was 2×10^4 Pa. Oxygen saturation was maintained by leaving the solution reservoirs open to the ambient atmosphere via air-permeable filters. Effluent solutions were sampled, filtered (0.4 μm), and analyzed for Pb by ICP-OES (ARL3520).

Because the initial solution did not contain dissolved Pb (or S), the dissolution rates of galena, R_{Pb}, (mol/m^2·s) were evaluated directly from the concentration of Pb in the output solution, (Pb^{2+}) by the following equation:

$$R_{Pb} = \left(Pb^{2+}\right)\frac{Q}{SA} \quad (1)$$

where SA is the amount of total surface area (m^2) in contact with solution. SA was determined as a geometric surface by measurement of the macroscopic grain surface and the microscopic roughness (estimated by AFM to be in the range 1.02–1.05 using Digital Instruments software). In these experiments, initial SA was between 2.8×10^{-5} and 3×10^{-5} m^2 (the grains are almost perfect parallelepipeds, with an edge length of 2 to 4 mm, and only one of the largest surfaces exposed to solution). The estimated error in SA is about 10%, while the intrinsic error in R_{Pb} is ±15%, mainly due to the uncertainty in SA.

Micro-Raman spectra (μRS) were collected in situ at room temperature with a triple Raman spectrometer (Dilor XY800) operating at the 514.5 nm line of an Argon ion laser (Coherent Innova 90C-4) in back-scattering geometry. Raman signal was collected through an Olympus microscope (BX-40, objective: 10×, numeric aperture 0.25), and dispersed using two different configurations: (1) single spectrometer coupled with a notch filter (Kaiser instruments) to remove the Rayleigh component and a spectral window of about 1500 cm^{-1} (direct dispersion system); (2) double monochromator in subtractive configuration coupled with the spectrometer to select a smaller spectral window and to collect the excited Raman spectra out to 30 cm^{-1} from the excitation wavelength. The Raman signal is stronger in the direct configuration, but the contribution of "out of focus" scattered light is higher, as well as the spectral background. The overall Raman efficiency depends mainly on the concentration of surface product species.

The gratings of the double monochromator have 1200 grooves/mm, and each grove is 500 nm depth. The spectrometer, also constituted by a 1200 grooves/mm grating, disperses the Raman signal onto a 1024 × 256 liquid nitrogen-cooled Charge Coupled Detector (CCD). The spectral resolution for both configurations was 1 cm^{-1}.

An inherent potential complication of Raman spectroscopy is laser-induced modification of the studied material. Specifically, the surface of galena undergoes a detectable photo-oxidation due to laser irradiation at high power density, with the appearance of peaks typical of the Pb-O bond (namely the formation of ortho-rhombic PbO; Batonneau et al. 2000) and of the S-O bond. Indeed, preliminary tests working with an excitation power density onto the sample of 500 W/mm^2 indicated that sulfate peaks appear in the Raman spectra after only 100 s of laser irradiation (Fig. 1a). To minimize any such thermal and/or photo-degradation effects, the laser power at the sample was kept as low as 25 mW, with a spot on the surface of 0.1 mm^2 (power density 0.25 W/ mm^2). For these conditions, only slight differences were observed between the spectra collected in air for a freshly cleaved surface (Fig 1b), and after 8 hours of continuous laser irradiation (Fig 1c). All the spectra from experiments in the fluid-cell were collected under this low laser power density, and the surface exposure to the laser beam was on the order of hundreds of seconds.

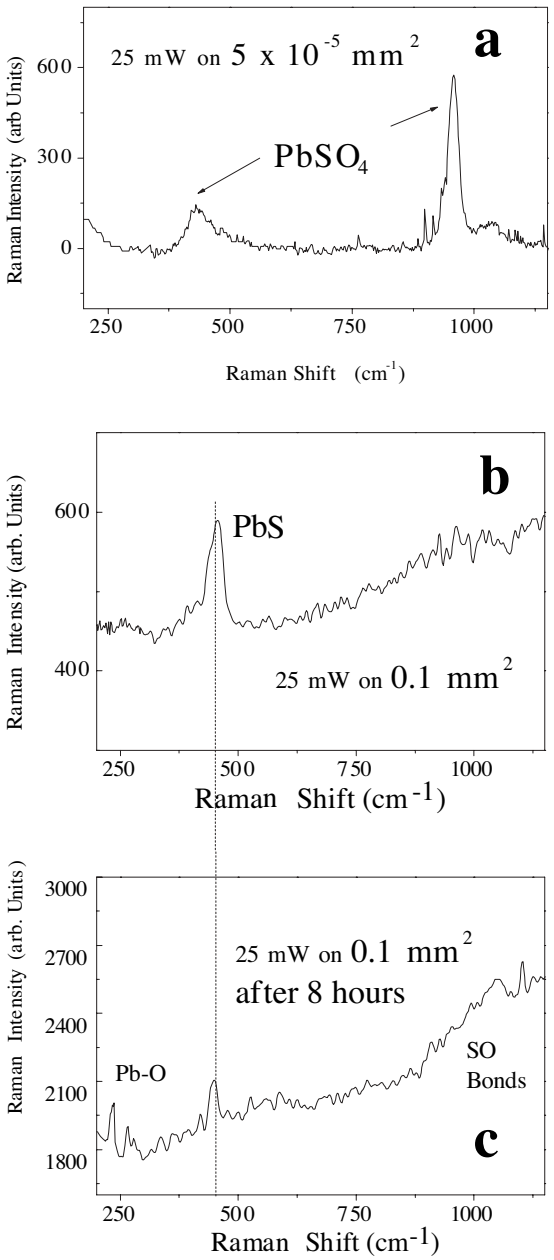

Figure 1. Galena surface in contact with ambient atmosphere. Raman spectra taken at two different excitation power densities: (**a**) 25 mW on 5×10^{-5} mm^2 = 500 W mm^2 power density, 100 s irradiation; (**b**) 25 mW on 0.1 mm^2 = 0.25 W mm^2 power density 100 s irradiation, and (**c**) after 8 hours of continuous excitation at 25 mW on 0.1 mm^2.

Results

During the experiments, several tens of Raman spectra of the reacting galena cleavage surface were collected for each pH condition at different reaction times. In addition, the position of

the laser beam (having an approximate cross section of 300 × 300 μm) was shifted by several hundreds of μm. Several peaks or bands were observed in these spectra. After spectral analysis, these peaks were assigned to specific vibrations/compounds on the basis of literature data, as detailed in Table 1. The μRS technique allows one to determine only the predominant surface species formed within a fairly thick and Raman-efficient surface coating. In addition, because the Raman efficiency depends on the crystallinity, and the thickness of surface coating can have spatial variability, μRS spectra can show some spatial variability. In this work, μRS spectra collected from different areas of a given surface at a given time showed occasional variability. The spectra shown hereafter are representative of all surface species detected.

Some compounds were clearly identified by some characteristic molecular vibration contained in the collected spectra. This is the case for crystalline sulfur (S-S vibration), $PbSO_4$, and crystalline PbO. Other compounds like sulfites (vibration SO_3^{2-}) and Pb hydroxide show less-intense specific vibrations, and their identification may be less certain. In addition, vibrations of some detected surface compounds, in contrast to the multiple reference peaks listed in Table 1, show only a single mode (i.e., stretching and bending of Pb-O and Pb-O-Pb; Pb-Cl).

A thorough examination of vibrational modes is not within the scope of this work, and can be found in the literature cited in Table 1. We wish to emphasize here the capability of μRS to discriminate among sulfur species that appear at dissolving galena surfaces. For instance, the pyramidal-shaped sulfite ion has only two Raman active modes. These appear as weak to moderate signals in the Raman spectrum at 933 and 964 cm^{-1} (see for instance the inset in Fig. 2a). The sulfate molecule is pyramidal shaped, too; however, its two totally symmetric-stretching modes show quite strong peaks in the Raman spectrum at 970 and 1010 cm^{-1}, whereas the other three modes give only a weak contribution, respectively at 1080–1100, 540–600, and 400–500 cm^{-1}. The thiosulfate ion ($S_2O_3^{2-}$) is similar to sulfate, showing a slightly distorted tetrahedral shape, with a central and a peripheral sulfur (S-SO_3). Therefore, the vibration modes active in the Raman spectrum are the same as those occurring for the SO_4^{2-} ion. The symmetric- and antisymmetric-stretching mode of the thiosulfate ion can be found at 1115–1120 and 980 cm^{-1} in PbS_2O_3, where Pb is O-coordinated. The other modes give only a weak contribution, not detected in our spectra. The sulfur dioxide molecule has only two symmetric-stretching modes in the Raman spectrum at 1100 and 1200 cm^{-1} (see, for instance, Fig. 2b). In conclusion, because the spectral resolution in our system is about 1 cm^{-1}, the presence of the above S species can be identified unambiguously by Raman spectra analysis.

TABLE 1. Main vibrational frequencies of relevant Pb-S-O-H-Cl species

Phases	Raman shifts (cm^{-1})	References
PbCl	130	Kammoun et al. (1996), Mirculescu (1974)
PbS	154; 210; 451*	Batonneau et al. (2000), Smith et al. (2002)
Pb-O	404; 228	Trettenhahn et al. (1993)
Pb-O-Pb	60; 87; 130*	Trettenhahn et al. (1993)
$PbSO_3$	950–1000	Chernyshova (2003)
SO_3^{2-}	950–960	
PbS_2O_3	982; 1115–1120	Chernyshova (2003)
$Pb(OH)_2$	1390–1396; 1007–1010	Chernyshova (2003), Jensen (2002)
PbO Tetragonal	180; 286 338*; 398; 1048;	Trettenhahn et al. (1993)
PbO Orthorombic	182; 286*; 380	Trettenhahn et al. (1993)
$PbSO_4$	182; 436; 450; 974*; 1057; 1154	Trettenhahn et al. (1993), Batonneau et al. (2000)
$PbO\text{-}PbSO_4\cdot H_2O$	957	Trettenhahn et al. (1993), Batonneau et al. (2000)
$PbO\cdot PbSO_4$	184*; 286; 965*	Trettenhahn et al. (1993), Batonneau et al. (2000)
SO_2	1100–1200; 1300–1400	Colthup et al. (1990)
S	150; 219*; 472*	McGuire et al. (2001) and references therein

* Diagnostic (strong) peaks.

Figures 2a, 2b, and 2c show the Raman spectra of dissolving galena cleavage surfaces under different conditions of solution composition after 24 hours of reaction. In particular, Figure 2a shows dissolution in deionized water at pH 5.8. For this pH condition, besides the PbS peaks, some additional peaks attributable to sulfites also can be recognized. The same behavior can be observed (Fig. 2b) for dissolution at pH 4.6 (HCl). However, the PbS peaks disappear for dissolution at pH 1 (HCl), and peaks corresponding to Pb-O bonds are clearly present in the spectra (Fig. 2c).

The spectra collected after 48 hours of reaction are shown in Figures 2d, 2e, and 2f. For the reaction with deionized water at pH 5.8, peaks ascribed to PbO and $PbSO_4$ are clearly recognizable (Fig. 2d). For the reaction with the pH 4.6 solution, the spectra indicate the presence of PbS and SO_3^{2-} (Fig. 2e). For the reaction at pH 1 (HCl), the spectra indicate the presence of orthorhombic PbO and $PbO\text{-}PbSO_4\cdot H_2O$ (Fig. 2f).

After 76 and 96 hours of reaction, the main difference in surface speciation with respect to shorter reaction times is the clear appearance of native sulfur at the dissolving surface at pH 1 (Figs. 2i and 2l). After 120 hours of reaction, the peaks of the dissolving surface at pH 5.8 are still ascribed to $PbSO_4$ and, probably, also to PbS_2O_3. Native S is the main species detected at the dissolving surface at pH 4.6. The same is true at pH 1 (native S was found in several spectra not shown in Fig. 2o), but some phase containing Pb-Cl bonds also appears (Fig. 2o).

The collected solution samples were analyzed for dissolved Pb and S, total S concentration was generally below the detection limit of our analytical techniques. The solution saturation state with respect to both galena and anglesite ($PbSO_4$) was calculated assuming that the concentration of total S is equal to the dissolved Pb concentration, and total dissolved sulfides represent ≤10% of total S. Solutions were always undersaturated with respect to these minerals, and the degree of undersaturation increased with the reaction time (see Table 2).

Dissolution rates are shown as function of time in Figure 3. It can be noted that the values decrease with reaction time, and all three apparently converge on nearly the same steady state value after about 40 hours. Such a trend of decreasing dissolution rates has been observed previously (see De Giudici and Zuddas 2001; De Giudici et al. 2005, and references therein). The dissolution rates at pH 1 in this study are in good agreement with those presented in De Giudici and Zuddas (2001). However, the dissolution rates reported in De Giudici et al. (2005) are higher by half an order of magnitude. As already discussed in De Giudici et al. (2005), the values of steady state dissolution rates depend

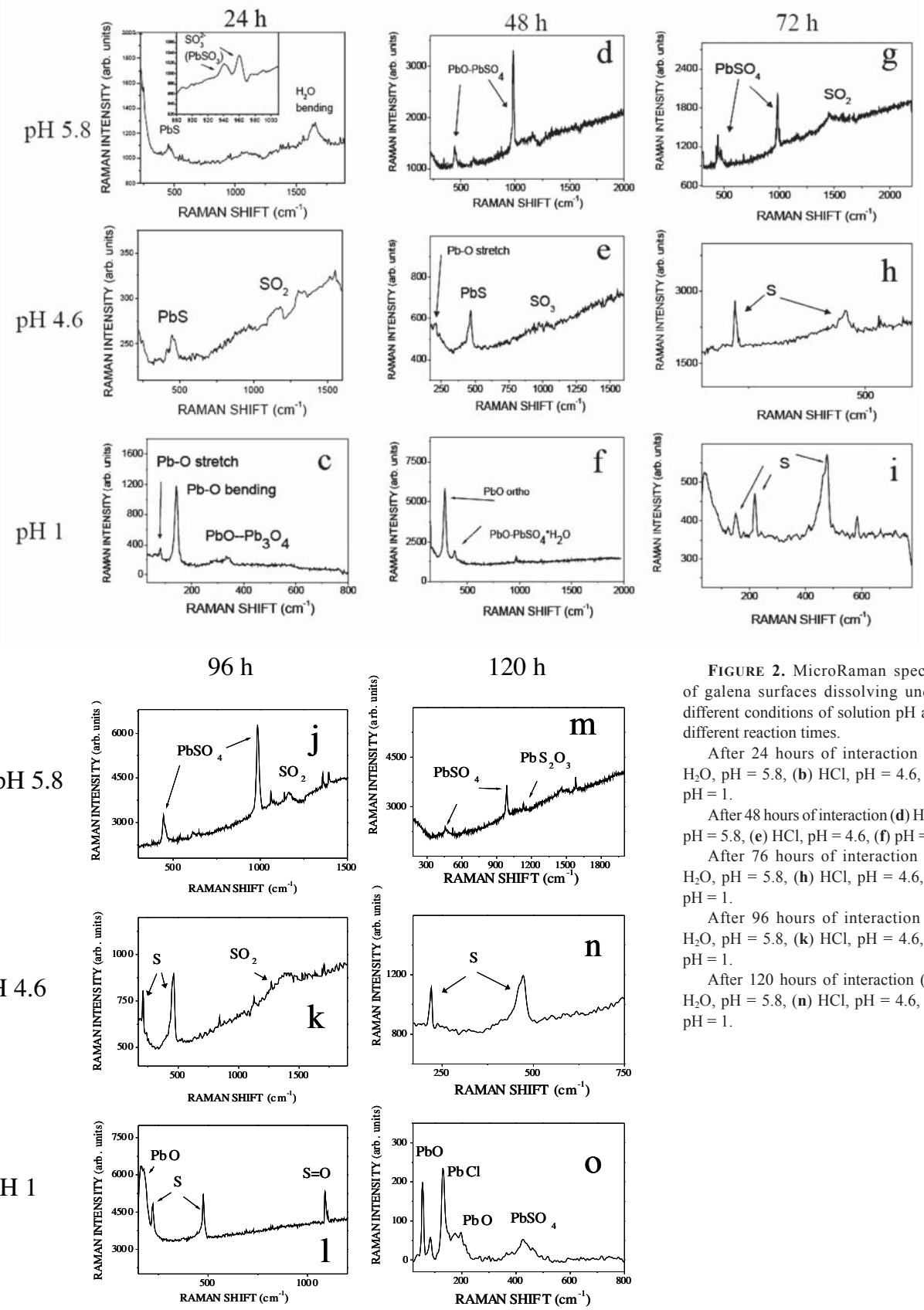

FIGURE 2. MicroRaman spectra of galena surfaces dissolving under different conditions of solution pH and different reaction times.

After 24 hours of interaction (**a**) H_2O, pH = 5.8, (**b**) HCl, pH = 4.6, (**c**) pH = 1.

After 48 hours of interaction (**d**) H_2O, pH = 5.8, (**e**) HCl, pH = 4.6, (**f**) pH = 1.

After 76 hours of interaction (**g**) H_2O, pH = 5.8, (**h**) HCl, pH = 4.6, (**i**) pH = 1.

After 96 hours of interaction (**j**) H_2O, pH = 5.8, (**k**) HCl, pH = 4.6, (**l**) pH = 1.

After 120 hours of interaction (**m**) H_2O, pH = 5.8, (**n**) HCl, pH = 4.6, (**o**) pH = 1.

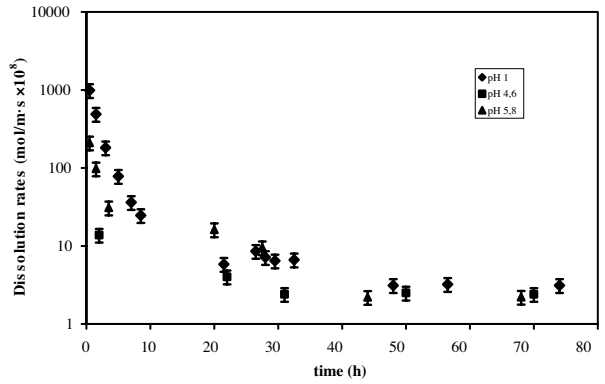

FIGURE 3. Dissolution rates (mol/m^2 s $\times$ 10^8) plotted as function of reaction time (hours).

on the reaction history, and can be influenced by hydrodynamics (i.e., the detailed manner in which the solution at the interface is renewed). Galena dissolution rates, in addition, can change by orders of magnitude depending on how the reactive surface is operatively defined (Cama et al. 2005). We suggest that the shape of the particular flow-through reactor can influence the measured dissolution rates, and is responsible for the difference between dissolution rates of this work and De Giudici and Zuddas (2001) and dissolution rates in De Giudici et al. (2005). It can be observed that during the experimental duration, dissolution rates decrease, while the undersaturation with respect to both galena and anglesite increases. Thus, the thermodynamic driving force is not the dissolution of galena and anglesite (see De Giudici and Zuddas 2001 for a more detailed discussion).

DISCUSSION

It often has been proposed that oxidative dissolution in acidic solutions takes place via an initial fast step of hydrogen ion adsorption onto the (001) galena surface, and then oxygen is adsorbed onto the surface. This leads to congruent dissolution as indicated by solution-chemistry measurements (Hsieh and Huang 1989) and is associated with the formation of Pb hydroxides and hydrogenated sulfide at dissolving galena surfaces (see Gerson and O'Dea 2003). In previous molecular-scale investigations using mainly AFM (De Giudici and Zuddas 2001; Stack et al. 2004; Cama et al. 2005; Mikhlin et al. 2005), the (001) galena surface was shown to react with oxygen-saturated solutions to form nanometer-sized phases that covered the surface. De Giudici and Zuddas (2001) addressed the issue that sulfur oxidation should partially take place at the interface, resulting in a local accumulation of matter, and then this surface accumulation will re-dissolve at a slower rate than galena. Given the typical errors in solution-chemistry measurements, however, the relatively small amount of matter accumulated as secondary phases often cannot be detected by this method. De Giudici et al. (2005) provided evidence for the presence of Pb-O bonds that also are compatible with Pb-OH phases. However, the data resulting from this µRS study clearly indicate the presence of Pb oxides rather than Pb hydroxides, in apparent contrast with postulated mechanisms of galena dissolution based on the dissociation of a water molecule during reaction with the surface. Computational modeling indicates that the S-O bond should be energetically favored over the Pb-O bond (Becker and Hochella 1996; Gerson and O'Dea 2003). This work indicated that several sulfoxy species can directly form at the dissolving surface. Based on both the literature and the present data, we propose that exchange of electrons during a redox reaction between dissolved molecular oxygen and exposed sulfur sites at the galena surface is one of the fundamental steps in the overall dissolution process. Based on µRS data, the interfacial process for the reaction at pH 1 and 4.6 can be represented as follows:

At pH 5.8, the process of sulfur oxidation appears to be different, and no significant amount of sulfur can oxidize to native sulfur. The interfacial process can then be represented as follows:

At the interface, along with sulfate species, thio-sulfate, traces of sulfites, and sulfur dioxide also can be found. In addition, the evidence for the presence of a compound containing Pb-Cl bonds at pH 1 implies that also a Pb-chloride surface complex may participate in the kinetics of galena dissolution, at least at relatively high chloride concentration. The formation of Pb-chloride complexes at the galena surface was suggested previously by Becker et al. (1997).

On the other hand, the observed secondary phases forming at the interface can be compared to the thermodynamic predictions based on an equilibrium approach. Several studies in the literature on the Eh-pH stability of galena (Sato 1992; Pourbaix and Pourbaix 1992, and references therein) predicted the formation of Pb sulfates, sulfur, and other metastable species of sulfur. Lead oxides (PbO and Pb_3O_4), however, are predicted to be stable only in contact with basic solutions. In fact, for Pb activities on the order of 10^{-5} (as found in the solutions flowing out from our fluid cell), Pb oxides (massicot and minium) cannot form in solutions with pH < 8.9. In addition, the presence of a soluble species such as sulfur dioxide is unexpected on the basis of equilibrium thermodynamics. This significant difference between thermodynamic predictions and detected surface speciation could be explained by: (1) a large local increase in oxygen and/or Pb activity at the interface with respect to their activity in the bulk solution; and/or (2) differences in the thermodynamic properties of the secondary nanophases with respect to their bulk counterparts; and/or (3) kinetic control favoring formation of thermodynamically unstable phases.

The µRS technique applied in the present work has a sampling depth on the order of several tens of nanometers and, thus, does not allow true molecular resolution of the surface processes. µRS can then be regarded as an in situ micrometer-scale technique that allows determination of predominant surface species. XPS measurements on the galena surface after protracted reaction with solutions at different pH values (Table 3) indicated that,

TABLE 2. Dissolution rates of galena, and saturation states, Ω, with respect to both galena and anglesite as a function of time at different pH

$\Omega_{galena} = \frac{[Pb^{2+}] \times [HS]}{[H^+] \times K_{sPbS}}$, $K_{sPbS} = 10^{12.75 \pm 0.17}$ $\Omega_{anglesite} = \frac{(Pb^{2+}) \times (SO_4^{2-})}{K_{sPBSP_4}}$,

$K_{sPbSO4} = 10^{-7.79 \pm 0.02}$

Time (h)	Pb^{2+} mol/L	Ω PbS	Ω $PbSO_4$	Dissolution rate mol m^{-2} s^{-1}
		pH 1		
74	1.5×10^{-7}	1.4×10^{-7}	1.4×10^{-6}	3.1×10^{-8}
56.5	1.5×10^{-7}	1.4×10^{-7}	1.5×10^{-6}	3.2×10^{-8}
48	1.5×10^{-7}	1.4×10^{-7}	1.4×10^{-6}	3.1×10^{-8}
32.5	3.2×10^{-7}	6.2×10^{-7}	6.4×10^{-6}	6.6×10^{-8}
29.5	3.1×10^{-7}	5.8×10^{-7}	6.0×10^{-6}	6.4×10^{-8}
28	3.4×10^{-7}	7.1×10^{-7}	7.4×10^{-6}	7.1×10^{-8}
26.5	4.1×10^{-7}	1.0×10^{-6}	1.1×10^{-5}	8.6×10^{-8}
21.5	2.8×10^{-7}	4.8×10^{-7}	4.9×10^{-6}	5.8×10^{-8}
8.5	1.2×10^{-6}	8.5×10^{-6}	8.8×10^{-5}	2.5×10^{-7}
7	1.7×10^{-6}	1.8×10^{-5}	1.9×10^{-4}	3.6×10^{-7}
5	3.8×10^{-6}	8.6×10^{-5}	8.8×10^{-4}	7.8×10^{-7}
3	8.7×10^{-6}	4.6×10^{-4}	4.8×10^{-3}	1.8×10^{-6}
1.5	2.3×10^{-5}	3.3×10^{-3}	3.4×10^{-2}	4.9×10^{-6}
		pH 4.6		
70	1.1×10^{-7}	6.8×10^{-8}	7.1×10^{-7}	2.5×10^{-8}
50	1.1×10^{-7}	6.8×10^{-8}	7.1×10^{-7}	2.5×10^{-8}
31	1.2×10^{-7}	8.8×10^{-8}	9.1×10^{-7}	2.9×10^{-8}
22	1.7×10^{-7}	1.7×10^{-7}	1.8×10^{-6}	4.0×10^{-8}
2	5.8×10^{-7}	2.0×10^{-6}	2.1×10^{-5}	1.4×10^{-7}
1.5	6.2×10^{-7}	2.3×10^{-6}	2.4×10^{-5}	1.5×10^{-7}
1	2.8×10^{-6}	4.8×10^{-5}	4.9×10^{-4}	6.7×10^{-7}
		pH 5.8		
68	9.7×10^{-8}	5.7×10^{-8}	5.8×10^{-7}	2.2×10^{-8}
44	9.7×10^{-8}	5.7×10^{-8}	5.9×10^{-7}	2.2×10^{-8}
27.5	4.1×10^{-7}	1.0×10^{-6}	1.1×10^{-5}	9.5×10^{-8}
20	7.0×10^{-7}	3.0×10^{-6}	3.1×10^{-5}	1.6×10^{-7}
3.5	1.3×10^{-6}	1.1×10^{-5}	1.1×10^{-4}	3.1×10^{-7}
1.5	4.3×10^{-6}	1.1×10^{-4}	1.1×10^{-3}	9.8×10^{-7}
0.5	9.1×10^{-6}	5.1×10^{-4}	5.2×10^{-3}	2.1×10^{-6}

at pH 5.8, surface coatings were made of Pb hydroxides and, probably, elemental sulfur (De Giudici et al. 2005). After reaction at pH 1.2 (HCl), the composition of the outermost layer also contained Pb oxides, with small amounts of sulfate and chloride, and possibly also metastable oxidized species such as thio-sulfates or sulfites (De Giudici et al. 2005). Thus there is a significant difference between XPS data and μRS data (see Fig. 2), and this could arise from two reasons. On the one hand, XPS and μRS instrumental techniques work, respectively, ex-situ and in-situ. As sulfur species like native sulfur, thiosulfates, and sulfites are metastable, the ex-situ measurements could result from artifacts due to sample manipulation (e.g., loss of volatile species in the high-vacuum XPS chamber; cf., Chernyshova and Andreev 1997). In addition, the sampling depth of XPS at the galena surface is generally limited to the outermost layers (nanometers), whereas the sampling depth of μRS is much higher. Thus, the differences between XPS and μRS data could largely arise from the difference in sampling depth and from the complexity of the structure of the galena-water interface and of the galena surface coating. In other words, if the formation of a small amount of native sulfur at the outermost layer of the galena cleavage surface dissolving at pH 5.8 occurs because of a disproportionation of thiosulfates or other intermediate sulfur species, it would be detected only by XPS.

The μRS technique can be profitably used to investigate other reactions of metal-sulfide minerals, where formation of a thick (several nanometers) surface layer coating of Raman-active species occurs. The experimental setup is comparatively simple, and allows in situ collection of chemical data at the micrometer-scale. The possibility of surface damage by laser irradiation can be minimized by a careful selection of the most appropriate excitation wavelength and power density at the surface. Finally, this microscale data collected by techniques such as μRS should be taken into account when scaling molecular information up to macroscopic behavior.

TABLE 3. Summary of the main species identified in this work, and comparison with XPS results of previous work on the same galena specimen

pH	24 h	48 h	72 h	96 h	120 h	650 h*
5.8	PbS Sulfites	PbO $PbSO_4$	PbO $PbSO_4$	PbO $PbSO_4$	$PbSO_4$ $PbSO_3$	PbOH S
4.6	PbS sulfites	PbS SO_3^{2-}	PbS SO_3^{2-}	PbS SO_3^{2-}	S	
1	PbO	PbO PbO-$PbSO_4$	S	S	S Pb-Cl	Pb-O Pb-Cl oxy/ hydrate/ sulfate

* XPS (De Giudici et al. 2005).

ACKNOWLEDGMENTS

This work was funded by MIUR (PRIN 2004, National coordinator: G. Artioli). The editorial handling of Andreas Luttge is appreciated. Two anonymous referees are acknowledged for their useful criticism and suggestions. Finally, the suggestions of Roy Wogelius were useful in order the improve the overall quality of this manuscript.

REFERENCES CITED

Andreev, G.N. and Barzev, A. (2003) Raman spectroscopic study of some chalcopyrite-xanthate flotation products. Journal of Molecular Structure, 661–662, 325–332.

Batonneau, Y., Brémard, C., Laureyns, J., and Merlin, J.C. (2000) Microscopic and imaging Raman scattering study of PbS and its photo-oxidation products. Journal of Raman Spectroscopy, 31, 1113–1119.

Becker, U. and Hochella, M.F. (1996) The calculation of STM images, STS spectra, and XPS peak shifts for galena: new tools for understanding mineral surface chemistry. Geochimica et Cosmochimica Acta, 60, 2413–2426.

Becker, U., Vaughan, D.J., and Hochella, M.F., Jr. (1997) The adsorption of gold to galena surfaces: Calculation of adsorption/reduction energies, reaction mechanisms, XPS spectra, and STM images. Geochimica et Cosmochimica Acta, 61, 3565–3585.

Cama, J., Acero, P., Ayora, C., and Lobo, A. (2005) Galena surface reactivity at acidic pH and 25 °C based on flow-through and in situ AFM experiments. Chemical Geology 214, 309–330

Chernyshova, I.V. (2003) An in situ FTIR study of galena and pyrite oxidation in aqueous solutions. Journal of Electrochemistry Analytical Chemistry, 558, 83–98.

Chernyshova, I.V. and Andreev, S.I. (1997) Spectroscopic study of galena surface oxidation in aqueous solutions I. Identification of surface species by XPS and ATR/FTIR spectroscopy. Applied Surface Science, 108, 225–236.

Colthup, N.B., Daly, L.H., and Wiberley, S.E. (1990) Introduction to infrared and Raman Spectroscopy (3rd edition). Academic Press, London.

De Giudici, G. and Zuddas, P. (2001) In situ investigation of galena dissolution in oxygen-saturated solutions: Evolution of surface features and kinetic rate. Geochimica et Cosmochimica Acta, 65, 1381–1389.

De Giudici, G., Rossi, A., Fanfani, L., and Lattanzi, P. (2005) Mechanisms of galena dissolution in oxygen-saturated solutions: evaluation of pH effect on apparent activation energies and mineral-water interface. Geochimica et Cosmochimica Acta, 69, 2321–2331.

Ferraro, J.R. (1975) Factor group analysis for some common minerals. Applied Spectroscopy, 29, 418–421.

Fornasiero, D., Fengsheng, L., Ralston, J., and Smart, R. (1994) Oxidation of galena surfaces. I. X-Ray photoelectron spectroscopic and dissolution kinetic studies. Journal of Colloids and Interface Science, 164, 333–344.

Gerson, A.R. and O'Dea, A. (2003) A quantum chemical investigation of the oxidation and dissolution mechanisms of Galena. Geochimica et Cosmochimica Acta, 67, 813–822.

Hsieh, Y.H. and Huang, C.P. (1989) The dissolution of $PbS_{(s)}$ in dilute aqueous solutions. Journal of Colloids and Interface Science, 131, 537–549.

Jensen, J.O. (2002) Vibrational frequencies and structural determinations of $Pb_4(OH)_4^{+}$. Journal of Molecular Structure, 587, 111–121.
Kammoun, S., Kamoun, M., Daoudy, A., and Lautie, A. (1996) Differential scanning calorimetric X-ray diffraction and spectroscopic studies of phase transitions in the bidimensional compound. Journal of Physics: Condensed Matter, 8, 8465–8476.
McGuire, M.M., Jallad, K.M., Ben-Amotz, D., and Hamers, R.J. (2001) Chemical mapping of elemental sulfur on pyrite and arsenopyrite surfaces using near-infrared Raman imaging microscopy. Applied Surface Science, 178, 105–115.
Mernagh, T.P. and Trudu, A.G. (1993) A laser Raman microprobe study of some geologically important sulphide minerals. Chemical Geology, 103, 113–127.
Mikhlin, Y.L., Romanchenko, A.S., and Shagaev, A.A. (2005) Scanning probe microscopy studies of PbS surfaces oxidized in air and etched in aqueous acid solutions. Applied Surface Science, 252, 5645–5658 (www.sciencedirect.com).
Mirculescu, L. (1974) Impurity-induced Raman spectra of KCl:Pb crystals. Journal of Physics C: Solid State Physics, 7, 2387–2390.
Nowak, P. and Laajalehto, K. (2000) Oxidation of Galena surface—an XPS study of the Formation of Sulfoxy Species. Applied Surface Science, 157, 1–11.
Pourbaix, M. and Pourbaix, A. (1992) Potential-pH equilibrium diagrams for the system S–H_2O from 25 to 150 °C: Influence of access in sulphide solutions. Geochimica et Cosmochimica Acta, 56, 3157–3178.
Sato, M. (1992) Persistency-field Eh-pH diagrams for sulfides and their application to supergene oxidation and enrichment of sulfide ore bodies. Geochimica et Cosmochimica Acta, 56, 3133–3156.
Shapter, J.G., Brooker, M.H., and Skinner, W.M. (2000) Observation of the oxidation of galena using Raman spectroscopy. International Journal of Mineral processing, 60, 199–211.
Smith, G.D., Firth, S., Clark, R.J.H., and Cardona, M. (2002) First- and second-order Raman spectra of galena (PbS). Journal of Applied Physics, 92, 4375–4380.
Stack, A.G., Erni, R., Browning, N.D., and Casey, W.H. (2004) Pyromorphite growth on lead-sulfide surfaces. Environmental Science and Technology, 38, 5529–5534.
Trettenhahn, G.L.J., Nauer, G.E., and Neckel, A. (1993) Vibrational Spectroscopy on the PbO-$PbSO_4$ System and some related Compounds Part 1: Fundamentals, infrared and Raman spectroscopy. Vibrational Spectroscopy, 5, 85–100.

Manuscript received December 7, 2005
Manuscript accepted October 12, 2006
Manuscript handled by Andreas Luttge